The Astrophysical Journal Supplement Series, 276:66 (13pp), 2025 February https://doi.org/10.3847/1538-4365/ada3c9

MARVEL Analysis of the Measured High-resolution Spectra of $^{12}C^{16}O$

Salman Mahmoud[1], Nayla El-Kork[1], Nariman Abu Elkher[1], Mubarak Almehairbi[2], Malathe Samir Khalil[3], Tibor Furtenbacher[4], Attila G. Császár[4], Olga P. Yurchenko[5], Sergey N. Yurchenko[5], and Jonathan Tennyson[5]
[1] Department of Physics, Khalifa University, Abu Dhabi, United Arab Emirates; nayla.elkork@ku.ac.ae
[2] Department of Chemistry, Khalifa University, Abu Dhabi, United Arab Emirates
[3] Department of Mechanical and Nuclear Engineering, Khalifa University, Abu Dhabi, United Arab Emirates
[4] Institute of Chemistry, ELTE Eötvös Loránd University, Pázmány Péter sétány 1/A, H-1117 Budapest, Hungary
[5] Department of Physics and Astronomy, University College London, London WC1E 6BT, UK; j.tennyson@ucl.ac.uk
Received 2024 October 12; revised 2024 December 18; accepted 2024 December 26; published 2025 February 5

Abstract

The Measured Active Rotational–Vibrational Energy Levels (MARVEL) algorithm is used to determine accurate empirical rotational–vibrational energy levels for the ground electronic state of the diatomic $^{12}C^{16}O$ molecule. 2293 energy levels have been obtained through a careful analysis of lines measured and assigned in high-resolution experimental spectra reported previously in 68 publications. Out of the 19,399 (7955) measured (unique) transitions in the limited wavenumber range of 0–14,470 cm^{-1}, an analysis of the resulting experimental spectroscopic network (SN) validates 19,219 (7795), and only 11 transitions had to be deleted from the SN assembled (note that transitions within floating components of the SN cannot be validated). The measured transitions span states with vibrational and rotational quantum numbers less than or equal to 41 and 123, respectively, with the highest validated energy level lying at 67,148.1 cm^{-1}. The validation procedure covers all transitions with a one-photon absorption intensity larger than 10^{-30} cm $molecule^{-1}$ at 296 K. The validated line centers and the empirical rovibrational energy levels of $^{12}C^{16}O$, with appropriate uncertainties and assignments, are provided in the appendix to this paper. Detailed comparisons are made with several existing data sets, such as the Kurucz and the HITRAN databases, NIST-certified wavelengths, and the list of lines protected by the International Astronomical Union, revealing occasional discrepancies.

Unified Astronomy Thesaurus concepts: Molecular spectroscopy (2095); Laboratory astrophysics (2004); Molecular physics (2058)

Materials only available in the online version of record: machine-readable tables

1. Introduction

Carbon monoxide, CO, is a molecule with a complex set of roles and impacts in a wide variety of astronomical environments; it is widely assumed to be the second most abundant molecule in the Universe, after H_2 (Y. Li et al. 1998; G. J. Vázquez et al. 2009). Following its initial discovery in interstellar space (R. W. Wilson et al. 1970), CO has been found in comets, planetary atmospheres, and photospheres of both the Sun and cooler stars (D. L. Cooper & K. P. Kirby 1987; R. Farrenq et al. 1991; F. Hase et al. 2010; V. A. Krasnopolsky 2014; P. F. Bernath 2016). Indeed, the band structure of the rotation–vibration spectrum of CO has proved to be particularly useful as a temperature diagnostic in the atmospheres of cool stars (H. R. A. Jones et al. 2005); a procedure which relies on the accurate determination of transitions involving states with highly excited rotational levels. The pure rotational and the rotational–vibrational spectra of carbon monoxide are particularly well studied in the interstellar medium (R. Gredel et al. 1987; W. W. Duley & D. A. Williams 1992), where they have often been used as proxies for the hard-to-observe H_2 molecule (N. Nakai & N. Kuno 1995). The first molecule detected in an exoplanet atmosphere, that of HD 189733b, using high-resolution spectroscopy was carbon monoxide (R. J. de Kok et al. 2013). Due to its distinctive properties, behavior, and importance in the probe of chemical and physical conditions in interstellar space, many experimental, theoretical, and computational studies on high-resolution spectra of carbon monoxide have been conducted.

During the past hundred years (E. F. Lowry 1924), numerous measurements, too many to be listed here, have been performed to determine the positions of the rovibrational and pure rotational lines of the $^{12}C^{16}O$ molecule (perhaps the first review of the band spectrum of CO was by P. H. Krupenie 1966). These measurements have been made under a variety of experimental conditions and they utilized various techniques, including grating interferometers, Fourier transform, and cavity ring-down spectroscopies, as well as Lamb dips, and heterodyne, microwave, and other setups. Several empirical analyses have also been performed to better understand the rovibrational states of $^{12}C^{16}O$ (T. I. Velichko et al. 2012, 2013; J. A. Coxon & P. G. Hajigeorgiou 2013). V. V. Meshkov et al. performed a series of studies based on the use of an explicit solution of the nuclear Schrödinger equation (V. V. Meshkov et al. 2018; E. S. Medvedev & V. G. Ushakov 2022; V. V. Meshkov et al. 2022); we compare with the results of V. V. Meshkov et al. (2022) below. HITRAN 2016 (I. E. Gordon et al. 2017), which we also discuss in the following, was updated based on the variational nuclear motion calculations of G. Li et al. (2015) using the potential energy curves of J. A. Coxon & P. G. Hajigeorgiou (2004). S. A. Tashkun et al. (2010) and T. I. Velichko et al. (2012, 2013) constructed a highly accurate set of Dunham coefficients for $CO(X^1\Sigma^+)$ using

data from various isotopologues, enabling predictions of the energy levels.

Rotational lines of several isotopologues of carbon monoxide are listed among the lines protected by the International Astronomical Union (IAU; National Academies of Sciences, Engineering and Medicine 2015). Eight of these lines belong to $^{12}C^{16}O$; two lines are below 300 GHz, the rest between 300 and 3000 GHz.

The National Institute of Standards (NIST) certifies, as Standard Reference Material (SRM) 2514 (S. L. Gilbert & W. C. Swann 2002), 41 lines of the 3ν band of $^{12}C^{16}O$ in the region of 1560–1630 nm and at a pressure of 1000 torr. The SRM 2514 data are based on vacuum wavelengths measured and tabulated for very low-pressure conditions with an uncertainty of approximately 8×10^{-6} nm (N. Picqué & G. Guelachvili 1997; W. C. Swann & S. L. Gilbert 2002). The SRM lines are certified wavelength references, with uncertainties ranging from 0.4 to 0.7 pm, which can be used in the optical fiber communication wavelength division multiplexing band *L*, the second lowest-loss wavelength band. Thanks to recent accurate measurements, it is worth comparing these data with the results of the present global analysis.

The triple-bonded CO molecule has a very high dissociation energy, more than 11 eV, and its two constituent atoms have a high abundance in the Universe. Thus, various spectral signatures and molecular emissions from highly excited rovibrational levels can be observed when studying astronomical sources, which may or may not be in local thermodynamic equilibrium, depending on temperature, pressure, velocity distribution, and especially the number of collisions per unit time; see, for example, R. R. Gamache et al. (2022). For the two most abundant isotopologues, $^{12}C^{16}O$ and $^{13}C^{16}O$, L. Goldberg & E. A. Müller (1953) analyzed solar lines with higher rotational excitation, reaching up to $J = 70$, where J is the rotational quantum number. They obtained sets of spectroscopic constants fitted to the observed line positions in both solar and stellar spectra. These constants were used in various spectroscopic compilations (W. S. Benedict et al. 1962) and astrophysical studies until the 1970s (J. Weinberg et al. 1965), when laboratory observations detected lines with even higher J values ($J \leqslant 94$; A. W. Mantz & J.-P. Maillard 1974).

D. H. Rank et al. (1965b) published experimental measurements of the rotational lines of the overtone bands of $^{12}C^{16}O$ using heated absorption tubes. These measurements were made with an uncertainty close to 0.003 cm^{-1}. In 1974, a high-resolution Fourier-transform spectrometer was used by A. W. Mantz & J.-P. Maillard (1974) for probing transitions of $^{12}C^{16}O$ within its electronic ground state ($X^1\Sigma^+$). They measured sequence bands for overtones with a difference of $\Delta v = 2$, where v is the vibrational quantum number. The R and P branches were observed up to $v' = 7$. Heterodyne frequency measurements of the 2–0 band of CO($X^1\Sigma^+$) were reported by C. R. Pollock et al. (1983), resulting in accurate line positions for the R and P branches and improved centrifugal distortion constants. In 1991, high-resolution spectra of CO and its isotopologues were extensively studied by R. Farrenq et al. (1991). Somewhat later, D. Goorvitch (1994) compiled a comprehensive theoretical line list for rovibrational transitions up to $v' = 22$. New data for the 3–0 band were presented by N. Picqué & G. Guelachvili (1997) and W. C. Swann & S. L. Gilbert (2002). Furthermore, A. P. Mishra et al. (2005), V. Malathy Devi et al. (2002), and V. Malathy Devi et al. (2004) reported measurements of several overtone bands (the $\Delta v = 2$ sequence) of $^{12}C^{16}O$, including numerous rovibrational transitions. The measurements of the 4–0 band by J. F. Ogilvie et al. (2002), the 5–0 band by C.-Y. Chung et al. (2005), and the 6–0 band by Y. Tan et al. (2017) followed. A. Cygan et al. (2016) achieved unprecedented accuracy in measuring the absolute frequencies of $^{12}C^{16}O$ transitions in the near-infrared 3–0 band, with relative uncertainties at the level of 10^{-10}. The CO (3–0) band's P-branch positions and line-shape parameters were measured with 70–420 kHz uncertainty, incorporating speed dependence and collision effects. Recently, A. A. Balashov et al. (2024) reported the measurement of the extremely weak (7–0) band of the $^{12}C^{16}O$ molecule, using a highly sensitive cavity ring-down spectrometer. This study provides a full set of line-shape parameters for 14 transitions, extending the experimental verification of pressure-shifting effects up to the sixth overtone.

A. Cygan et al. (2019) developed frequency-based molecular dispersion spectroscopy, achieving subhertz precision and sub-per-mille accuracy, crucial for error-free gas detection. This method offers a sensitivity of 5×10^{-11} cm^{-1} and high speed, enabling comprehensive molecular spectroscopy without setup modifications. K. Bielska et al. (2021) introduced frequency-based cavity mode-dispersion spectroscopy to saturation spectroscopy, highlighting its advantages over traditional intensity-based methods. Their CO second overtone transition frequency measurements have uncertainties below 500 Hz, thus a relative uncertainty of $<3 \times 10^{-12}$, and they were able to detect previously unseen Lamb-dip pressure shifts.

In this paper, we are considering all the measured and assigned frequencies, ranging from the microwave to the visible region, 3.8–14,470 cm^{-1}, reported in the literature for the electronic ground state of $^{12}C^{16}O$. Both nuclei have zero spin, simplifying the analysis of the measured spectra. Using the Measured Active Rotational–Vibrational Energy Levels (MARVEL) algorithm (A. G. Császár et al. 2007; T. Furtenbacher et al. 2007; T. Furtenbacher & A. G. Császár 2012a), described in some detail in Section 2.1, accurate empirical rovibrational energy levels are obtained. These empirical rovibrational energy levels, strictly based on measured transitions, allow the representation of all one-photon room-temperature transitions with an intensity greater than 10^{-30} cm $molecule^{-1}$.

This paper is organized as follows. Section 2 presents an overview of the method used to create the MARVEL database, which includes measured rovibrational transitions and empirical energy levels of the ground electronic state of $^{12}C^{16}O$. A review of the large number of experimental sources included in the MARVEL database is also provided in Section 2, along with a brief description of the procedure used for data treatment, followed by a discussion providing comments on each data source. The results, discussion, and comparison with other studies, as well as with the T. I. Velichko et al. (2012), V. V. Meshkov et al. (2022), and Kurucz databases, are given in Section 3. In Section 4, we present the summary and conclusions of this study.

2. Methodological Details

2.1. MARVEL

MARVEL (A. G. Császár et al. 2007; T. Furtenbacher et al. 2007; T. Furtenbacher & A. G. Császár 2012; R. Tóbiás et al. 2019; J. Tennyson et al. 2024) is an algorithm that converts a

Table 1
$^{12}C^{16}O$ Data Sources; the Tags Provide Partial Provenance, and their Characteristics, including the Number of Measured (A), Validated (V), and Deleted (D) Transitions

Source Tag	Range (cm^{-1})	$A/V/D$	CSU	MSU
77Dixon (T. Dixon 1977)	3.78–3.81	2/2/0	5.0×10^{-6}	5.0×10^{-6}
57GoCo (W. Gordy & M. Cowan 1957)	3.85–11.53	3/3/0	3.0×10^{-6}	3.0×10^{-6}
58RoNeTo (B. Rosenblum et al. 1958)	3.85	1/1/0	1.7×10^{-7}	1.7×10^{-7}
85WiWiWi (M. Winnewisser et al. 1985)	3.85–19.22	5/5/0	4.3×10^{-7}	4.3×10^{-7}
96MaGuDoNi (H. Mäder et al. 1996)	3.85	1/1/0	6.7×10^{-8}	6.7×10^{-8}
97WiBeKlSc (G. Winnewisser et al. 1997)	3.85–23.07	6/6/0	1.7×10^{-8}	1.7×10^{-8}
86BoDeDeLa (M. Bogey et al. 1986)	4.88–7.34	31/31/0	6.7×10^{-7}	6.7×10^{-7}
09GeLeKlMe (R. Gendriesch et al. 2009)	7.55–64.65	21/21/0	9.6×10^{-7}	9.6×10^{-7}
92BeTrSu (S.-P. Belov et al. 1992)	7.69–15.38	3/3/0	4.4×10^{-8}	4.4×10^{-8}
70HeDeGo (P. Helminger et al. 1970)	11.53–26.91	5/5/0	2.0×10^{-6}	2.4×10^{-6}
95BeLeKlWi (S. P. Belov et al. 1995)	11.53–42.26	6/6/0	1.7×10^{-7}	1.7×10^{-7}
64JoGo (G. Jones & W. Gordy 1964)	15.38–23.07	3/3/0	8.5×10^{-6}	9.7×10^{-6}
02MaGoSa (V. N. Markov et al. 2002)	19.22	1/1/0	1.7×10^{-7}	1.7×10^{-7}
87NoRaDiEv (I. G. Nolt et al. 1987)	19.22–129.77	7/7/0	3.1×10^{-6}	3.6×10^{-6}
92VaEv (T. D. Varberg & K. M. Evenson 1992)	23.07–144.77	26/26/0	4.6×10^{-7}	5.9×10^{-7}
95Evenson (K. Evenson 1995)	26.91–144.77	22/22/0	4.7×10^{-7}	4.7×10^{-7}
83GuDeFaUr (G. Guelachvili et al. 1983)	1159.53–6335.42	5060/5054/0	9.0×10^{-4}	9.2×10^{-4}
74RoNa (W. B. Roh & K. N. Rao 1974)	1209.89–2012.74	227/227/0	5.0×10^{-3}	6.1×10^{-3}
70Yardley (J. T. Yardley 1970)	1215.71–2012.70	213/213/0	4.8×10^{-2}	5.2×10^{-2}
87HiWeMa (A. Hinz et al. 1987)	1257.40–1334.91	13/13/0	1.0×10^{-4}	1.0×10^{-4}
89ScEvVaJe (M. Schneider et al. 1989)	1257.40-1931.41	140/140/0	6.4×10^{-5}	6.4×10^{-5}
85WeHiMa (J. S. Wells et al. 1985)	1284.17–1339.93	8/8/0	1.0×10^{-4}	1.0×10^{-4}
21PaCiCl (A. Pastorek et al. 2021)	1330.25–4342.20	2409/2392/0	1.0×10^{-3}	1.9×10^{-3}
91FaGuSaGr (R. Farrenq et al. 1991)	1367.02–5858.92	6581/6436/0	1.4×10^{-3}	1.4×10^{-3}
70MaNiAl (A. W. Mantz et al. 1970)	1424.63–1986.92	194/188/6	6.9×10^{-3}	1.3×10^{-2}
76ToClTe (T. R. Todd et al. 1976)	1637.14–2254.75	761/761/0	1.4×10^{-3}	1.8×10^{-3}
74KiEnRo (H. Kildal et al. 1974)	1779.16–1957.05	22/22/0	1.4×10^{-4}	2.6×10^{-4}
74EnKiMiSp (R. S. Eng et al. 1974)	1880.90–1957.05	7/7/0	1.3×10^{-4}	1.4×10^{-4}
54PlBlCo (E. K. Plyler et al. 1955)	1905.78–2224.69	58/58/0	2.0×10^{-2}	2.0×10^{-2}
60RaSkEa (D. H. Rank et al. 1961)	1905.78–4342.20	65/65/0	3.4×10^{-3}	6.3×10^{-3}
70SoSaOs (D. R. Sokoloff et al. 1970)	1935.48	1/1/0	1.8×10^{-3}	2.0×10^{-3}
79Guelachv (G. Guelachvili 1979)	1958.60–2271.35	136/136/0	3.9×10^{-4}	5.1×10^{-4}
90ScWeMa (M. Schneider et al. 1990)	1995.11–2081.26	25/25/0	1.0×10^{-4}	1.0×10^{-4}
90MaWeJe (A. G. Maki et al. 1990)	2008.53–2154.60	2/2/0	2.2×10^{-4}	2.2×10^{-4}
98DeBeSmRi (V. M. Devi et al. 1998)	2008.53–2247.03	63/63/0	1.6×10^{-4}	1.7×10^{-4}
85BrTo (L. R. Brown & R. A. Toth 1985)	2055.40–2131.63	12/12/0	1.0×10^{-5}	1.4×10^{-5}
94GeSaWaUr (T. George et al. 1994)	2056.05–2111.54	14/14/0	2.0×10^{-6}	2.0×10^{-6}
97WaSaMeGe (M. H. Wappelhorst et al. 1997)	2056.05–2111.54	14/14/0	2.0×10^{-6}	2.0×10^{-6}
14NgLaPa (N. H. Ngo et al. 2014)	2059.91–2212.63	40/40/0	1.9×10^{-4}	1.9×10^{-4}
91GeWuDa (T. George et al. 1991)	2086.32	1/1/0	1.7×10^{-6}	3.1×10^{-6}
61RaEaRaWi (D. H. Rank et al. 1961)	2094.86–2161.97	11/11/0	5.0×10^{-3}	5.0×10^{-3}
05MiShKs (A. P. Mishra et al. 2005)	2122.76–4357.85	1547/1541/6	5.3×10^{-3}	9.4×10^{-3}
65WeFiRa (J. Weinberg et al. 1965)	2176.57–2290.91	193/193/0	8.4×10^{-3}	1.6×10^{-2}
74MaMa (A. W. Mantz & J.-P. Maillard 1974)	3764.74–4360.10	629/629/0	1.0×10^{-3}	1.9×10^{-3}
65RaPiWi (D. Rank et al. 1965a)	3992.20–4359.85	146/146/0	3.5×10^{-3}	5.1×10^{-3}
83PoPeJeWe (C. R. Pollock et al. 1983)	4120.73–4350.72	20/20/0	1.9×10^{-4}	1.9×10^{-4}
02DeBeSm (V. Malathy Devi et al. 2002)	4132.15–4338.76	55/55/0	1.4×10^{-4}	2.8×10^{-4}
17EsPrPo (K. Esteki et al. 2017)	4148.80–4328.88	47/47/0	5.0×10^{-4}	7.8×10^{-4}
15MoSaKaRo (D. Mondelain et al. 2015)	6176.11–6417.81	107/107/0	2.7×10^{-5}	3.5×10^{-5}
21WaHuLi (J. Wang et al. 2021)	6183.14–6416.30	61/61/0	6.8×10^{-7}	6.9×10^{-7}
13WoStMa (S. Wójtewicz et al. 2013)	6203.10–6210.25	4/4/0	1.6×10^{-3}	1.6×10^{-3}
02SwGi (W. C. Swann & S. L. Gilbert 2002)	6259.59–6408.20	14/14/0	1.9×10^{-4}	2.6×10^{-4}
97PiGu (N. Picqué & G. Guelachvili 1997)	6270.91–6405.09	36/36/0	3.0×10^{-5}	3.3×10^{-5}
17KoStWa (G. Kowzan et al. 2017)	6287.12–6342.64	5/5/0	5.4×10^{-6}	9.2×10^{-6}
20NiKoCh (A. Nishiyama et al. 2020)	6325.80–6334.43	2/2/0	1.3×10^{-4}	1.8×10^{-4}
99HeSiMo (J. Henningsen et al. 1999)	6354.18–6406.70	21/21/0	1.0×10^{-2}	1.0×10^{-2}
21BiCyKo (K. Bielska et al. 2021)	6377.41–6385.77	2/2/0	1.4×10^{-8}	1.4×10^{-8}
92YoSa (T. Yoshida & H. Sasada 1992)	6385.77–6388.35	2/2/0	4.8×10^{-4}	5.0×10^{-4}
19CiWcWo (A. Cygan et al. 2019)	6410.88	1/1/0	6.7×10^{-7}	6.7×10^{-7}
16CyWoKoZa (A. Cygan et al. 2016)	6412.06–6415.67	2/2/0	4.5×10^{-6}	4.5×10^{-6}
15CaKaKa (A. Campargue et al. 2015)	8206.15–8317.64	15/15/0	1.0×10^{-4}	2.2×10^{-4}

Table 1
(Continued)

Source Tag	Range (cm^{-1})	$A/V/D$	CSU	MSU
21BoKaCa (B. Bordet et al. 2021)	8206.15–8464.88	114/114/0	1.7×10^{-3}	1.8×10^{-3}
15LiGoRo (G. Li et al. 2015)	8206.16–8317.64	12/12/0	1.3×10^{-3}	1.3×10^{-3}
02OgChLeSa (J. F. Ogilvie et al. 2002)	8311.16–8464.86	46/46/0	1.2×10^{-3}	1.5×10^{-3}
49HeNa (G. Herzberg & K. N. Rao 2004)	8330.18–8460.74	36/36/0	9.2×10^{-3}	1.3×10^{-2}
05ChOgLe (C.-Y. Chung et al. 2005)	10,356.32–10,439.90	16/16/0	1.2×10^{-1}	2.6×10^{-1}
17TaWaZhLi (Y. Tan et al. 2017)	12,347.17–12,493.49	32/32/0	7.4×10^{-4}	9.7×10^{-4}
24BaWoDo (A. A. Balashov et al. 2024)	14,334.40–14,469.23	14/14/0	3.4×10^{-4}	3.9×10^{-4}

Note. Shown is the claimed source uncertainty (CSU) and the average MARVEL-suggested source uncertainty (MSU).

set of measured and uniquely assigned transition frequencies to a set of empirical energy levels. MARVEL provides well-defined uncertainties for the energy levels, carried over from the input transition data. The inversion process is based on the creation of a well-connected spectroscopic network (SN; A. G. Császár & T. Furtenbacher 2011; T. Furtenbacher & A. G. Császár 2012b; T. Furtenbacher et al. 2014; P. Árendás et al. 2016), based on a collection of experimental data with proper provenance and quantified uncertainties. In the SN the energy levels are the vertices, and the transitions form the set of edges. In this work, the final uncertainties of the empirical rovibrational energies are determined using a bootstrap procedure (J. Tennyson et al. 2024). To learn more about the MARVEL algorithm and the related software, see T. Furtenbacher & A. G. Császár (2012b) and A. G. Császár et al. (2016).

The MARVEL approach has been used to deduce empirical energy levels for isotopologues of astronomically important molecules, including $^{12}C_2$ (T. Furtenbacher et al. 2016), acetylene (K. L. Chubb et al. 2018), SO_2 (R. Tóbiás et al. 2018), ammonia (A. R. Al Derzi et al. 2015; T. Furtenbacher et al. 2020), H_2S (K. L. Chubb et al. 2018), and isotopologues of H_3^+ (T. Furtenbacher et al. 2013a, 2013b; C. A. Bowesman et al. 2023). There are several additional studies, for example, for the isotopologues of water (J. Tennyson et al. 2009, 2010, 2013, 2014a), for which the MARVEL workflow was originally developed (J. Tennyson et al. 2014b).

Based on the empirical energy levels and their uncertainties, transitions can be generated, which can then be compared to the measured transitions of the input file. In this way, it is possible to pinpoint inconsistencies in the input data, which may arise due to various factors, such as misassignments, underestimated uncertainties, and typographical or digitization errors. To remedy these issues, the MARVEL input transition list is increased gradually, moving from more accurately measured transitions to less well known ones, and issues are resolved as new transitions are added. Transitions initially discarded in this process may be reconsidered later on.

The set of validated transitions, those that are consistent with all the energies extracted from the original data set, can be compared to the input transitions, determining minimum, average, and maximum uncertainties for the transition frequencies. Usually, we utilized the minimum uncertainty obtained from the original experimental paper, or our own approximation, as the initial input uncertainty. If it is observed that the average uncertainty significantly exceeds the minimum uncertainty, the minimum uncertainty for the whole data set increases, and another MARVEL analysis is started.

In this paper, the MARVEL algorithm was employed using the code MARVELOnline, accessible at http://kkrk.chem.elte.hu/marvelonline. During this study, multiple minor improvements to the online interface were implemented to improve the speed, simplicity, and accuracy of data processing. For example, users can now choose to update the uncertainties automatically when processing initial data to obtain a self-consistent SN, as soon as certain thresholds are reached.

2.2. Quantum Numbers

The MARVEL algorithm relies on uniquely labeled transitions to determine the corresponding empirical energy levels. Although MARVEL does require unique descriptors for each state, it treats the descriptors simply as a set of characters. The physical correctness of these labels does not affect the validity of the inversion procedure. However, using appropriate and physically motivated labels is beneficial, for example, for making comparisons with other data sets and for identifying problems. In the case of the $^{12}C^{16}O$ molecule, all rovibrational energy levels were labeled using two physically motivated descriptors: the vibrational and the rotational quantum numbers, v and J, respectively.

2.3. Characteristics of the Data Collected

There are several papers reporting high-accuracy measurements of rovibrational transition frequencies for the parent isotopologue of carbon monoxide, $^{12}C^{16}O$. At the beginning of our study, we conducted a thorough and careful search for all relevant high-resolution spectroscopic data that could be utilized, including transition frequencies, their corresponding uncertainties, and the assignments for both the upper and the lower states. To provide complete provenance of the input data, each transition was given a unique reference tag. The notation used for the data source tag was based on a method adopted by an IUPAC Task Group dedicated to water spectroscopy (J. Tennyson et al. 2010; J. Tennyson et al. 2014b).

The uncertainties associated with the transition frequencies were primarily taken from the experimental data sources; however, sometimes uncertainties had to be adjusted to achieve self-consistency for the given version of the data set. To rationalize the increases in the uncertainties, we note that many of the sources providing high-resolution spectroscopic data give uncertainty estimates that are correct only for the strongest, well-separated lines in a vibrational band. For this reason, the authors may underestimate the true uncertainty that should be associated with some or all of the weaker lines, especially those lines that are blended.

Table 1 lists all sources that reported measured lines with rotational resolution and which were collected and utilized in the MARVEL analysis of this study. Table 1 also provides

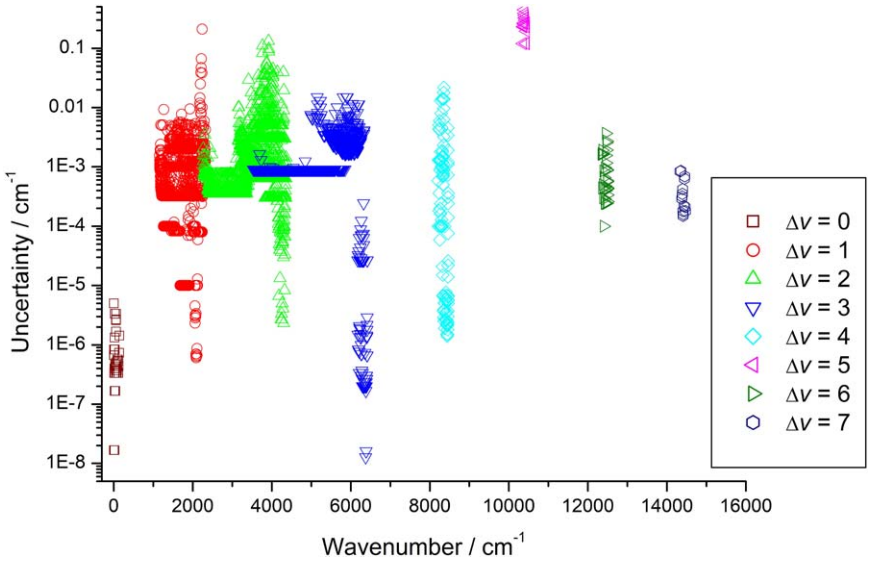

Figure 1. Uncertainties of the experimental rovibrational measurements available for $^{12}C^{16}O$, as a function of the transition wavenumber. The most accurate transition is chosen if there are multiple measurements. The entries are colored according to the vibrational excitation, Δv. In this transition data set the largest change during a measured rovibrational transition is $\Delta v = 7$.

information about the uncertainties that characterize each source. In total, 68 data sources were utilized during this study, which contained 19399 rovibrational transitions (the number of unique transitions, 7955, is significantly smaller). Levels associated with a total of 42 vibrational states were analyzed. For the bands investigated the maximum change in the vibrational quantum number is $\Delta v = 7$ (see Figure 1). Figure 1 clearly demonstrates that the wavenumber ranges covered by the measurements are rather limited and explains why in the limited range of the experiments, 0–14,470 cm^{-1}, there are transitions involving high-energy states, up to 67,148 cm^{-1}. The complete set of transitions utilized during this study can be found in the Appendix to this paper.

2.4. Comments on Data Sources Given in Table 1

During the MARVEL process, several of the estimated uncertainties taken from the original sources had to be changed to establish a self-consistent SN. Remarks concerning Table 1, largely regarding the uncertainty initially selected, are as follows.

74RoNa. S. A. Tashkun et al. (2010) and T. I. Velichko et al. (2012) confirm that self-consistency is achieved with an uncertainty of 5×10^{-3} cm^{-1}; therefore, we adopted this value for all lines.

70Yardley. Our estimated uncertainty of 5×10^{-3} cm^{-1} provided self-consistency for most transitions.

74MaMa, 83GudeFa, 91FaGuSa, 91GeWuDa, and 70MaNiAl. Data were obtained from the compilation given by T. I. Velichko et al. (2012), while the estimated uncertainties of 1–6 $\times 10^{-3}$ cm^{-1} were taken from S. A. Tashkun et al. (2010). It was necessary to eliminate two transitions reported in 70MaNiAl (A. W. Mantz et al. 1970).

95Evenson. Data were obtained from T. I. Velichko et al. (2012), who give uncertainties of 5×10^{-2} MHz, which we adopted.

70HeDeGo. For consistency with other measurements, an uncertainty of 6×10^{-2} MHz was adopted for all lines.

97WaSaMe. The stated uncertainties are in the range of 9.0×10^{-4}–4.8×10^{-2} MHz; however, we found it necessary to increase these uncertainties to 0.1 MHz for consistency with other measurements.

85BrTo. This work is unspecific about individual line uncertainties; we adopted a value of 1.0×10^{-5} cm^{-1} for all lines based on consistency within our overall data set.

17TaWaZh. The stated uncertainties were between 1.1 and 9×10^{-6} cm^{-1}; however, we found that an uncertainty of 5×10^{-5} cm^{-1} for all the transitions agrees more consistently with other measurements.

15CaKaKa. The stated uncertainties were between 1×10^{-5} and 1×10^{-4} cm^{-1}; however, to be consistent with T. I. Velichko et al. (2012) we adopted an uncertainty of 1×10^{-4} cm^{-1} for all transitions.

17EsPrPo. The stated uncertainties are in the range of 1.0–9.9 $\times 10^{-5}$ cm^{-1}; however, we found significant inconsistencies with this uncertainty and increased it to 1.0×10^{-4} cm^{-1} for all lines.

57GoCo. We were unable to obtain a copy of this paper; data were obtained from T. I. Velichko et al. (2012) and given uncertainties of 2×10^{-4} cm^{-1} for all transitions.

77Dixon. Data were obtained from T. I. Velichko et al. (2012), where two transitions were given with an uncertainty of 2×10^{-4} cm^{-1}, which we adopted.

97OgChLe. The stated uncertainties were 1×10^{-5} cm^{-1}; however, we found that a higher uncertainty of 5×10^{-4} cm^{-1} was necessary for consistency within this source and with results from other sources.

21PaCiCl. No uncertainty is given; however, 1×10^{-3} cm^{-1} is a reasonable choice, providing consistency for most transitions. Note that these are satellite bands and, hence, had lower intensities and higher positional uncertainties than the main bands.

02OgChLe. No uncertainties are given; however, 8.8×10^{-4} cm^{-1} appears to be a reasonable estimate for most transitions.

05MiShKs. The stated uncertainties ranged from 1.0×10^{-4} to 4.5×10^{-2} cm^{-1}; however, we found that an uncertainty of 5×10^{-3} cm^{-1} was required for consistency both within the source and with respect to other measurements. Five lines from this source had to be deleted.

Table 2
Sources of Rovibrational Data for $^{12}C^{16}O$ Not Used in the Present MARVEL-based Study

Tag	Reference	Comment
73Guelachv	G. Guelachvili (1973)	Only calculated values are given.
04MaCrBe	V. Malathy Devi et al. (2004)	Data appear to be taken from C. R. Pollock et al. (1983).
04CoBe	J. A. Coxon & P. G. Hajigeorgiou (2004)	Data appear to be taken from C. R. Pollock et al. (1983).
20BoSoSoPe	Y. G. Borkov et al. (2020)	Calculated values only.

65RaPiWi. An uncertainty of 1×10^{-3} cm^{-1} is stated; we adopted uncertainties of 0.003 and 0.004 cm^{-1}, depending on the band, to achieve consistency with other sources.

54PlBlCo. We adopted an uncertainty of 0.02 cm^{-1}, which gives self-consistency with other results.

There are a few other experimental high-resolution spectroscopic studies of $^{12}C^{16}O$ which we are aware of, but did not use. These data sources are listed in Table 2, with comments explaining why they have been left out.

3. Results and Discussion

3.1. MARVEL Energy Levels

During this study, 2293 empirical rovibrational energy levels have been determined for the electronic ground state of $^{12}C^{16}O$. By convention MARVEL sets the zero of energy as the $(v, J) = (0, 0)$ level meaning that it does not include a contribution from the zero-point energy. Table 3 provides a succinct summary of the characteristics of these levels. Figure 2 shows the energies as a function of the rotational quantum number J for the various rovibrational states. The smooth, quadratic shape of the curves reflects the reliability of the energy levels extracted through MARVEL, at least on the scale of the figure.

Table 3 gives the average uncertainties and the range of energy levels the MARVEL analysis of this study yielded. It should be added that the minimum uncertainty is usually significantly smaller than the average one, often less than 10^{-4} cm^{-1}, while the maximum uncertainty may exceed 0.1 cm^{-1}, which is generally true for high-J states.

Table 3
Certain Characteristics of the 2293 Empirical Rovibrational Energy Levels Determined during the Present MARVEL Analysis for the Ground Electronic State of $^{12}C^{16}O$

v	J Range	Avg. Unc.	Range of Energy Levels
0	0–120	0.0036	0.000–26,640.731
1	0–121	0.0037	2143.271–28,947.927
2	0–122	0.0038	4260.062–31,222.784
3	0–121	0.0036	6350.439–32,637.421
4	0–122	0.0039	8414.469–34,850.800
5	0–123	0.0040	10,452.222–37,031.838
6	0–118	0.0037	12,463.768–36,790.334
7	0–115	0.0036	14,449.181–37,381.891
8	0–110	0.0036	16,408.535–37,267.651
9	0–107	0.0035	18,341.905–37,926.732
10	0–105	0.0031	20,249.368–38,945.739
11	0–100	0.0029	22,131.005–38,983.130
12	0–88	0.0031	23,986.895–37,025.462
13	0–84	0.0030	25,817.120–37,608.712
14	0–77	0.0025	27,621.762–37,476.985
15	0–76	0.0026	29,400.905–38,906.529
16	0–60	0.0023	31,154.634–37,084.799
17	0–60	0.0022	32,883.031–38,749.208
18	0–53	0.0021	34,586.184–39,137.351
19	0–44	0.0022	36,264.176–39,388.935
20	0–39	0.0015	37,917.093–40,355.809
21	0–30	0.0014	39,545.015–40,986.241
22	0–29	0.0014	41,148.029–42,481.404
23	0–30	0.0014	42,726.215–44,134.956
24	0–29	0.0014	44,279.654–45,582.634
25	0–30	0.0014	45,808.423–47,184.671
26	0–29	0.0012	47,312.596–48,585.171
27	0–30	0.0014	48,792.246–50,135.973
28	0–27	0.0013	50,247.442–51,327.362
29	0–28	0.0013	51,678.248–52,823.661
30	0–27	0.0013	53,084.723–54,138.144
31	0–21	0.0011	54,466.923–55,103.435
32	0–20	0.0011	55,824.897–56,396.275
33	0–22	0.0012	57,158.686–57,837.875
34	0–20	0.0012	58,468.326–59,024.900
35	0–20	0.0012	59,753.844–60,302.991
36	0–19	0.0012	61,015.259–61,505.464
37	0–19	0.0012	62,252.580–62,736.025
38	0–19	0.0015	63,465.805–63,942.466
39	0–14	0.0013	64,654.921–64,914.807
40	0–14	0.0016	65,819.904–66,076.008
41	2–12	0.0016	66,967.931–67,148.195

Note. The energies and average uncertainties (avg. unc.) are in units of cm^{-1}, and v and J are the vibrational and rotational quantum numbers, respectively.

3.2. Comparison with Different Data Sources

3.2.1. Pure Rotational Lines

Probably it is the source T. I. Velichko et al. (2012) that provides the most accurate effective Hamiltonian parameters, defining the rotational lines of the $^{2012}C^{16}O$ molecule; therefore, we used these data to verify our MARVEL results in the microwave region. Three important observations can be made with respect to Table 4, which contains the results of this comparison.

First, with one exception, all experimentally measured frequencies can be reproduced, within experimental uncertainty, using the MARVEL energy levels. The $J' = 10 \leftarrow J'' = 9$ transition cannot be reproduced, as the J. Wang et al. (2021) measurements, accurate to the kHz level, significantly influence the values of the $J = 9$ and $J = 10$ rotational energy levels. Second, when considering the uncertainties of the MARVEL energy levels, it is straightforward to determine up to which J value a high-precision SN for the $^{12}C^{16}O$ molecule can be constructed, as the uncertainty of the $J' = 35 \leftarrow J'' = 34$ transition is an order of magnitude greater than that of the lower J-value transitions. Third, it is evident that the discrepancy between the present MARVEL and the T. I. Velichko et al. (2012) results is significant only in those cases where no direct experimental measurements are available for the given transition.

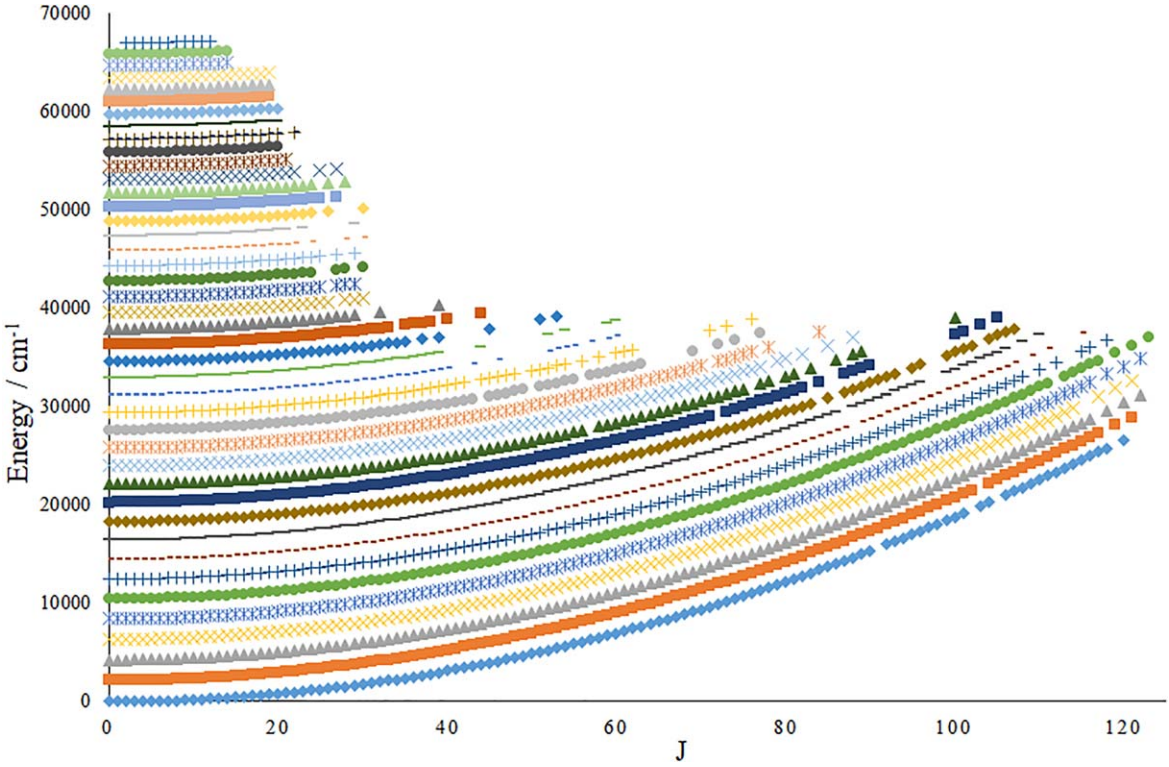

Figure 2. Pictorial representation of the empirical rovibrational energy levels of $^{12}C^{16}O$ determined in this study as a function of the J rotational quantum number and the vibrational states (different colors refer to different vibrational states).

3.2.2. Comparison with the Kurucz Database (R. L. Kurucz et al. 2009)

The Kurucz database (R. L. Kurucz et al. 2009) of the $^{12}C^{16}O$ molecule contains 396,629 rovibrational lines in the 1000–10,376 cm^{-1} region. At first sight, it may be somewhat surprising that the transitions predicted by MARVEL in this region account for only 3.6% of the transitions present in the Kurucz database. This highlights the fact that many energy levels remain unknown, as they have not been involved in measured transitions. Figure 3 shows the differences between the MARVEL-predicted wavenumbers and those of the Kurucz database. In most cases the deviations are less than 0.005 cm^{-1}, but there are several transitions where the deviations exceed 0.01 cm^{-1}; each of these transitions has a high J value ($J > 100$) or a high v value ($v > 25$).

3.2.3. Comparison with V. V. Meshkov et al. (2022)

MARVEL databases of validated transitions and empirical energy levels have traditionally been compared with the corresponding entries of the HITRAN database. In the case of $^{12}C^{16}O$, this would have meant a comparison with the 1344 rovibrational transitions present in the HITRAN 2020 (I. E. Gordon et al. 2022) database. However, instead of the HITRAN 2020 data set, we made the comparison with the semiempirical line list reported in V. V. Meshkov et al. (2022), since these line positions are on average better than those in HITRAN 2020, with the exception where frequency-comb data were used directly. Note also that in about 75% of the cases the present study provides transition data significantly more accurate than those in HITRAN 2020 (I. E. Gordon et al. 2022).

The database of V. V. Meshkov et al. (2022) contains 75,697 rovibrational lines in the 2.4–12,496.9 cm^{-1} region. Only 32% of the V. V. Meshkov et al. (2022) lines can be predicted using the empirical (MARVEL) energy levels. Figure 4 shows the result of a comparison between the MARVEL and the V. V. Meshkov et al. (2022) transition wavenumbers. In most cases the wavenumber differences are less than 0.001 cm^{-1}, but here again there are a few transitions for which the differences are larger than 0.01 cm^{-1}. All of these transitions were published by A. Pastorek et al. (2021) and belong to very high vibrational bands ($v > 27$).

3.2.4. The Most Intense Lines of $^{12}C^{16}O$ at Room Temperature

The line list of V. V. Meshkov et al. (2022) contains 950 rovibrational transitions, in the 2.4–12,496.9 cm^{-1} region, with intensities higher than 1×10^{-30} cm $molecule^{-1}$ at room temperature; we note that this source appears to be complete at even significantly lower intensities than 1×10^{-30} cm $molecule^{-1}$. Nine hundred and fifty is a small number of transitions, leading to two relevant questions: (a) is the HITRAN 2020 database complete in the sense that it contains all the lines strong enough to be important for atmospheric studies, and (b) can all the relatively intense lines of $^{12}C^{16}O$ (those stronger than 1×10^{-30} cm $molecule^{-1}$ at 296 K) be predicted using the MARVEL rovibrational energy levels?

The answer to the first question is that the HITRAN 2020 database is complete: it contains all the atmospherically important rovibrational lines of $^{12}C^{16}O$ with intensities greater than 1×10^{-30} cm $molecule^{-1}$ at 296 K. Furthermore, the average deviation between the wavenumbers of V. V. Meshkov et al. (2022) and the wavenumbers of HITRAN 2020 is 3×10^{-5} cm^{-1}; thus, without exception, the agreement is perfect.

Table 4
Observed and Calculated Pure Rotational Frequencies of $^{12}C^{16}O$, with $J'' = 0$–49

J'	J''	ν (Obs.)	ν (NASEM)	ν (12VeMiTa Calc).	ν (MARVEL)	ν (12VeMiTa Calc.) − ν (MARVEL)	ν (Obs.) − ν (MARVEL)
1	0	115,271.2018(5)	115,271	115,271.2022	115,271.2019(5)	0.3	0.1
2	1	230,538.0000(5)	230,538	230,538.0003	230,538.0000(5)	0.3	0.0
3	2	345,795.9899(5)	345,796	345,795.9902	345,795.9901(5)	0.1	0.2
4	3	461,040.7682(5)	461,041	461,040.7683	461,040.7682(5)	0.1	0.0
5	4	576,267.9305(5)	576,268	576,267.9312	576,267.9305(5)	0.7	0.0
6	5	691,473.0763(5)	691,473	691,473.0759	691,473.0763(5)	0.4	0.0
7	6	806,651.8060(50)	806,652	806,651.8003	806,651.8044(50)	4.1	1.6
8	7	921,799.7000(50)	921,800	921,799.7029	921,799.7005(50)	2.4	0.5
9	8	1,036,912.3930(50)	1,036,912	1,036,912.3830	1,036,912.3920(50)	9.0	1.0
10	9	1,151,985.4520(110)	1,151,985	1,151,985.4410	1,151,985.4385(1360)	2.5	13.5
11	10	1,267,014.4860(50)	1,267,014	1,267,014.4785	1,267,014.4840(50)	5.5	2.0
12	11	1,381,995.1050(130)	1,381,995	1,381,995.0982	1,381,995.0991(130)	0.9	5.9
13	12	1,496,922.9090(120)	1,496,923	1,496,922.9042	1,496,922.9057(120)	1.5	3.3
14	13	1,611,793.5180(110)	1,611,794	1,611,793.5021	1,611,793.5119(110)	9.8	6.1
15	14	1,726,602.4700(780)	1,726,603	1,726,602.4992	1,726,602.4929(260)	6.3	22.9
16	15	1,841,345.5060(110)	1,841,346	1,841,345.5045	1,841,345.5090(110)	4.5	3.0
17	16	1,956,018.1390(110)	1,956,018	1,956,018.1288	1,956,018.1370(110)	8.2	2.0
18	17	2,070,615.9930(140)	2,070,616	2,070,615.9848	2,070,615.9913(140)	6.5	1.7
19	18	2,185,134.6800(130)	2,185,135	2,185,134.6875	2,185,134.6825(130)	5.0	2.5
20	19	2,299,569.8420(100)	2,299,569	2,299,569.8540	2,299,569.8444(100)	9.6	2.4
21	20	2,413,917.1130(110)	2,413,924	2,413,917.1038	2,413,917.1150(110)	11.2	2.0
22	21	2,528,172.0600(110)	2,528,166	2,528,172.0587	2,528,172.0596(110)	0.9	0.4
23	22	…	2,642,321	2,642,330.3433	2,642,330.3348(838)	8.5	…
24	23	2,756,387.5840(170)	2,756,383	2,756,387.5846	2,756,387.5850(170)	0.4	1.0
25	24	2,870,339.4070(130)	2,870,338	2,870,339.4127	2,870,339.4087(130)	4.0	1.7
26	25	2,984,181.4550(140)	2,984,168	2,984,181.4604	2,984,181.4568(140)	3.6	1.8
27	26	3,097,909.3610(170)		3,097,909.3635	3,097,909.3626(170)	0.9	1.6
28	27	…		3,211,518.7611	3,211,518.7763(1251)	15.2	…
29	28	…		3,325,005.2955	3,325,005.2570(1291)	38.5	…
30	29	3,438,364.6110(100)		3,438,364.6121	3,438,364.6133(100)	−1.2	2.3
31	30	3,551,592.3610(100)		3,551,592.3602	3,551,592.3619(100)	1.7	0.9
32	31	…		3,664,684.1923	3,664,681.1795(11382)	3012.8	…
33	32	3,777,635.7280(160)		3,777,635.7647	3,777,635.7295(160)	35.2	1.5
34	33	3,890,442.7170(130)		3,890,442.7375	3,890,442.7210(130)	16.5	4.0
35	34	…		4,003,100.7746	4,003,101.4017(149,967)	627.1	…
36	35	4,115,605.5850(220)		4,115,605.5440	4,115,605.5885(520)	44.5	3.5
37	36	…		4,227,952.7176	4,227,953.5982(271,780)	880.6	…
38	37	4,340,138.1120(430)		4,340,137.9717	4,340,138.1180(530)	146.3	6.0
39	38	…		4,452,156.9866	4,452,148.3791(384,180)	8607.5	…
40	39	…		4,564,005.4471	4,564,007.5345(469,904)	−2087.4	…
41	40	…		4,675,679.0425	4,675,671.3528(475,885)	7689.7	…
42	41	…		4,787,173.4665	4,787,173.3621(520,744)	104.4	…
43	42	…		4,898,484.4176	4,898,481.4998(562,129)	2917.8	…
44	43	…		5,009,607.5990	5,009,600.5902(623,841)	7008.8	…
45	44	…		5,120,538.7185	5,120,550.4849(658,535)	11,766.4	…
46	45	…		5,231,273.4890	5,231,257.5285(691,651)	15,960.5	…
47	46	…		5,341,807.6283	5,341,806.5972(723,323)	1031.1	…
48	47	…		5,452,136.8592	5,452,143.3996(753,576)	6540.4	…
49	48	…		5,562,256.9097	5,562,256.5167(800,586)	393.0	…
50	49	…		5,672,163.5129	5,672,153.4161(827,966)	10,096.8	…

Note. All frequency values are in units of MHz and all differences are in units of kHz. The 2σ uncertainties of the transitions are given in parentheses. ν (NASEM) are rotational frequencies under protection by the National Academies of Sciences, Engineering, and Medicine (NASEM).

The answer to the second question is also yes, which means that the empirical rovibrational energy list obtained in this study contains all the levels needed to calculate the atmospherically important lines of $^{12}C^{16}O$. The average deviation between the predicted wavenumbers of MARVEL and the wavenumbers of V. V. Meshkov et al. (2022) is 7×10^{-5} cm^{-1}; thus, the agreement is perfect once again.

3.2.5. Lines of $^{12}C^{16}O$ Protected by the IAU

Table 4 contains $^{12}C^{16}O$ rotational lines protected by certain bodies of the NASEM (National Academies of Sciences, Engineering and Medicine 2015). As seen there, below 2.4 THz the NASEM data show good agreement with the experimental, calculated (T. I. Velichko et al. 2012), and

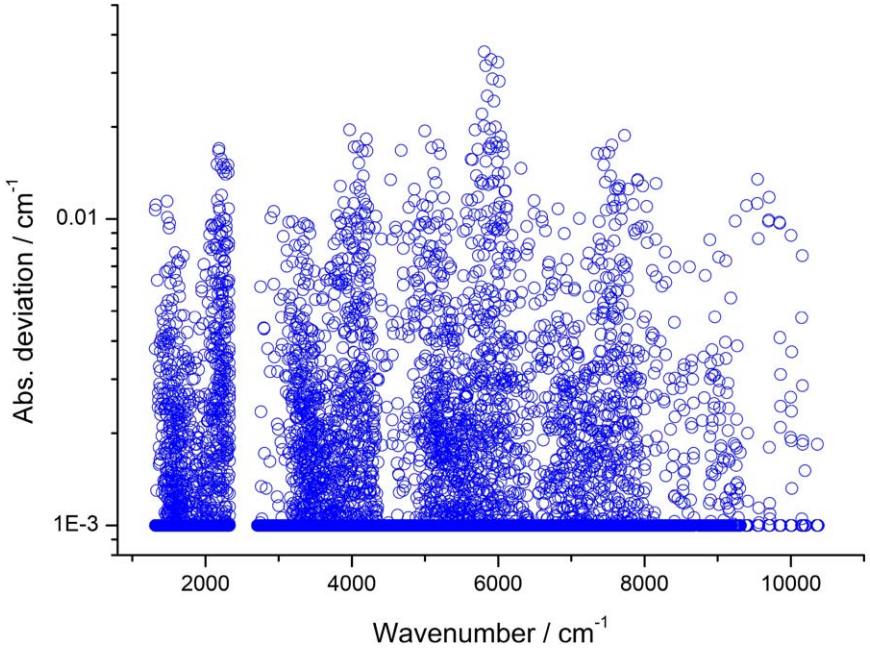

Figure 3. Absolute deviations between rovibrational transitions predicted by the present MARVEL analysis and those of the Kurucz database.

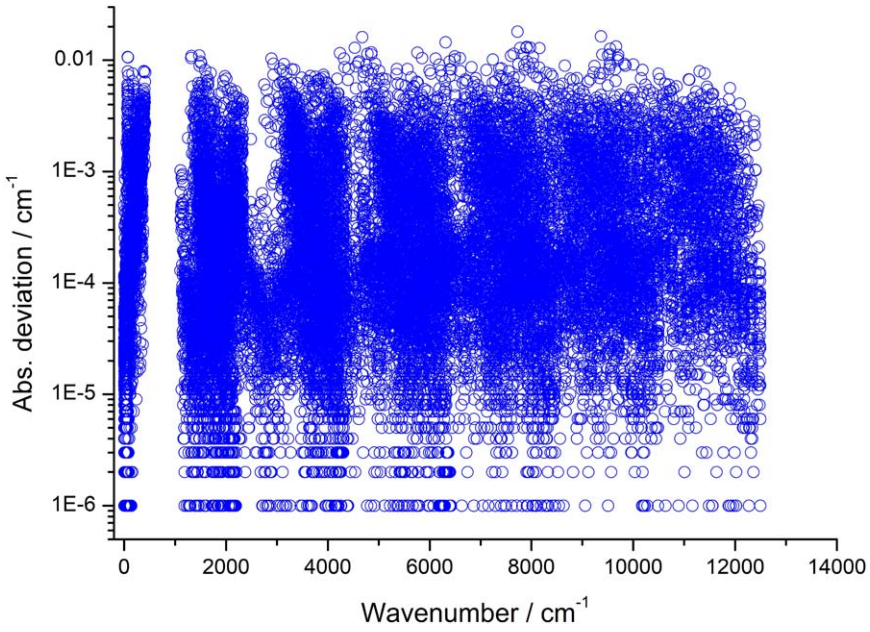

Figure 4. Absolute deviations between the rovibrational transitions predicted by the present MARVEL analysis and those of V. V. Meshkov et al. (2022).

empirical (MARVEL) results. However, above 2.4 THz, there are discrepancies up to several megahertz; thus, we suggest checking these data and recommend the experimental (or calculated) data for future use. Note that above 3 THz, where there are no IAU-protected lines, significant differences can be observed between the data of T. I. Velichko et al. (2012) and those of the present analysis.

3.2.6. Accuracy of Lines Used for Calibration

Table 5 contains the SRM 2514 NIST certified (S. L. Gilbert & W. C. Swann 2002) wavelengths (at 133 kPa), the corresponding extrapolated wavenumbers at zero pressure, and the empirical (MARVEL) wavenumbers of the 3ν band of $^{12}C^{16}O$. Clearly, in a considerable number of cases, there are differences of 1–2 $\times$ 10^{-4} cm^{-1} between the highly accurate lines of the present study and the zero-pressure lines of SRM 2514.

4. Summary and Conclusions

We have compiled a database that includes all measured, assigned, and publicly available rovibrational transitions of the parent, $^{12}C^{16}O$ isotopologue of carbon monoxide. By applying the MARVEL protocol to the SN of 19,399 transitions collected from 68 sources, of which 7955 are unique, we

Table 5
NIST Certified Wavelengths (S. L. Gilbert & W. C. Swann 2002), the Corresponding Wavenumbers Extrapolated to Zero Pressure ($\tilde{\nu}$), and Empirical (MARVEL) Wavenumbers of Lines of the 3ν Band of $^{12}C^{16}O$

Line	Wavelength at 133 kPa (nm^{-1})	$\tilde{\nu}$ at Zero Pressure (cm^{-1})	$\tilde{\nu}$ (MARVEL) (cm^{-1})	$\tilde{\nu}$ at Zero Pressure − $\tilde{\nu}$(MARVEL) (cm^{-1})
R21	1560.5025	6408.2025	6408.2024940(21)	0.0000
R20	1560.8680	6406.7016	6406.7015489(20)	0.0001
R19	1561.2600	6405.0927	6405.0925172(20)	0.0002
R18	1561.6786	6403.3754	6403.3755457(13)	–0.0001
R17	1562.1237	6401.5506	6401.5507804(11)	–0.0002
R16	1562.5953	6399.6182	6399.6183674(10)	–0.0002
R15	1563.0935	6397.5784	6397.5784527(10)	–0.0001
R14	1563.6183	6395.4312	6395.4311826(8)	0.0000
R13	1564.1697	6393.1766	6393.1767035(8)	–0.0001
R12	1564.7477	6390.8150	6390.8151617(6)	–0.0002
R11	1565.3523	6388.3466	6388.3467032(6)	–0.0001
R10	1565.9835	6385.7715	6385.7714748(5)	0.0000
R9	1566.6414	6383.0898	6383.0896227(4)	0.0002
R8	1567.3261	6380.3012	6380.3012937(4)	–0.0001
R7	1568.0375	6377.4065	6377.4066339(2)	–0.0001
R6	1568.7756	6374.4056	6374.4057902(2)	–0.0002
R5	1569.5405	6371.2988	6371.2989092(2)	–0.0001
R4	1570.3323	6368.0860	6368.0861374(2)	–0.0001
R3	1571.1509	6364.7677	6364.7676217(2)	0.0001
R2	1571.9965	6361.3436	6361.3435088(2)	0.0001
R1	1572.8691	6357.8140	6357.8139455(2)	0.0001
R0	1573.7687	6354.1791	6354.1790787(2)	0.0000
P1	1575.6498	6346.5939	6346.5940217(2)	–0.0001
P2	1576.6311	6342.6439	6342.6441253(2)	–0.0002
P3	1577.6397	6338.5897	6338.5895129(2)	0.0002
P4	1578.6758	6334.4301	6334.4303315(2)	–0.0002
P5	1579.7392	6330.1666	6330.1667279(2)	–0.0001
P6	1580.8300	6325.7990	6325.7988492(2)	0.0002
P7	1581.9485	6321.3267	6321.3268421(3)	–0.0001
P8	1583.0945	6316.7509	6316.7508539(3)	0.0000
P9	1584.2683	6312.0710	6312.0710312(3)	0.0000
P10	1585.4698	6307.2877	6307.2875212(5)	0.0002
P11	1586.6993	6302.4005	6302.4004707(5)	0.0000
P12	1587.9567	6297.4101	6297.4100263(5)	0.0001
P13	1589.2422	6292.3164	6292.3163353(6)	0.0001
P14	1590.5559	6287.1195	6287.1195438(7)	0.0000
P15	1591.8978	6281.8198	6281.8197992(8)	0.0000
P16	1593.2681	6276.4172	6276.4172479(8)	0.0000
P17	1594.6669	6270.9118	6270.9120358(9)	–0.0002
P18	1596.0942	6265.3042	6265.3043104(11)	–0.0001
P19	1597.5502	6259.5942	6259.5942181(12)	0.0000

could validate 7795 unique transitions. This enabled us to establish a set of 2293 empirical rovibrational energy levels with well-defined uncertainties. The empirical rovibrational energy levels on the ground electronic state of $^{12}C^{16}O$ thus established span the range of 0–68,000 cm^{-1}. Note that the active nature of the MARVEL protocol means that the $^{12}C^{16}O$ MARVEL input file can be easily updated in the future by incorporating new spectroscopic data, giving an improved and/or extended set of MARVEL energies with a revised set of uncertainties.

The transitions and empirical rovibrational energy levels determined in this study were compared with the corresponding data of T. I. Velichko et al. (2012), V. V. Meshkov et al. (2012), and the Kurucz database (R. L. Kurucz et al. 2009). Using data from T. I. Velichko et al. (2012), the MARVEL frequencies of the pure rotational band (0–0) of $^{12}C^{16}O$ were checked up to $J = 50$. Discrepancies between the present MARVEL and the results of T. I. Velichko et al. (2012) are significant only in those cases where direct experimental measurements are not available. Comparison of our data with those of V. V. Meshkov et al. (2012) shows that in most cases the differences in wavenumbers are less than 0.001 cm^{-1}, and there are only a few transitions for which the differences are greater than 0.01 cm^{-1}. A comparison with the Kurucz database leads to two important conclusions: (a) the average difference is about 0.005 cm^{-1}, and (b) the Kurucz database contains orders of magnitude more transitions, highlighting that many energy levels of $^{12}C^{16}O$ remain unknown as they have not been involved in experimentally measured transitions.

Finally, it is noted that significant progress has been made in constructing theoretical models that give highly accurate transition intensities for CO (K. Bielska et al. 2022; A. A. Balashov et al. 2023). These intensities can be combined with the accurate empirical energies reported here to give a highly accurate line list for $^{12}C^{16}O$.

Acknowledgments

The authors thank Prof. Roman Ciuryło and Dr. Iouli Gordon for helpful responses to their queries. This work was supported by Khalifa University of Science and Technology under Award No. CIRA-2019-054 and the Aspire Award for Research Excellence (AARE), Award No. 000-329-00001, as well as the European Research Council (ERC) under the European Union's Horizon 2020 research and innovation program through Advance Grant 883830 (ExoMolHD). The work carried out in Budapest received support from the National Research, Development, and Innovation Office (NKFIH, grant no. K138233). This publication supports coordinated research efforts performed within the COST Action CA21101 "Confined molecular systems: from a new generation of materials to the stars" (COSY), funded by the European Cooperation in Science and Technology (COST), and the MSCA Doctoral Network PHYMOL, "Physics, Accuracy and Machine Learning: Toward the Next Generation of Molecular Potentials."

Data Availability

The data underlying this article are available in the article and in the associated machine-readable tables.

Appendix
MARVEL Files

The MARVEL input and output files are given in machine-readable form in this appendix. Tables 6, 7, and 8 contain extracts of the input transitions, the segment file, and the output energies file, respectively. Note that the purpose of the segment file is to provide the units in which the transitions are recorded and listed in the input.

Table 6
MARVEL Transitions File

ν (cm^{-1})	$u_{initial}$ (cm^{-1})	u_{final} (cm^{-1})	v'	J'	v''	J''	Tag
8418.1310000	0.032	0.044	4	1	0	0	49HeNa.1
8421.7280000	0.001	0.011	4	2	0	1	49HeNa.2
8425.1580000	0.004	0.006	4	3	0	2	49HeNa.3
8428.4400000	0.001	0.008	4	4	0	3	49HeNa.4
8431.5770000	0.006	0.015	4	5	0	4	49HeNa.5
8434.5850000	0.002	0.009	4	6	0	5	49HeNa.6
8437.4530000	0.004	0.004	4	7	0	6	49HeNa.7

Note. ν is the wavenumber entry for the transition, $u_{initial}$ and u_{final} are the initial and final uncertainties of the transition, respectively, v and J are the vibrational and rotational quantum numbers, respectively, of the initial ($''$) and final ($'$) states, while tag refers to the source of the transition.

(This table is available in its entirety in machine-readable form in the online article.)

Table 7
MARVEL Segments File

Tag	Unit
02MaBeSmRi	cm^{-1}
02MaGoSa	MHz
02OgChLeSa	cm^{-1}
02SwGi	cm^{-1}
05ChOgLe	cm^{-1}
05MiShKs	cm^{-1}
09GeLeKlMe	MHz

(This table is available in its entirety in machine-readable form in the online article.)

Table 8
MARVEL Energy Levels File

v	J	E (cm^{-1})	Uncertainty (cm^{-1})	N
0	0	0.000000000	0.00	32
0	1	3.845033415	16.7×10^{-9}	56
0	2	11.534953354	23.6×10^{-9}	62
0	3	23.069466010	28.9×10^{-9}	59
0	4	38.448130680	33.4×10^{-9}	65
0	5	57.670359764	37.3×10^{-9}	59
0	6	80.735418869	40.9×10^{-9}	60

Note. v and J are the vibrational and rotational quantum numbers, respectively, E is the empirical rovibrational energy level determined through a MARVEL analysis, while N is the number of incident transitions.

(This table is available in its entirety in machine-readable form in the online article.)

ORCID iDs

Nayla El-Kork https://orcid.org/0000-0002-5402-4951
Sergey N. Yurchenko https://orcid.org/0000-0001-9286-9501
Jonathan Tennyson https://orcid.org/0000-0002-4994-5238

References

Al Derzi, A. R., Furtenbacher, T., Tennyson, J., Yurchenko, S. N., & Császár, A. G. 2015, JQSRT, 161, 117
Árendás, P., Furtenbacher, T., & Császár, A. G. 2016, JMaCh, 54, 806
Balashov, A. A., Bielska, K., Li, G., et al. 2023, JChPh, 158, 234306
Balashov, A. A., Wójtewicz, S., Domysławska, J., et al. 2024, AcSpA, 312, 124041
Belov, S. P., Lewen, F., Klaus, T., & Winnewisser, G. 1995, JMoSp, 174, 606
Belov, S.-P., Tret'iakov, M. I., & Suenram, R.-D. 1992, ApJ, 393, 848
Benedict, W. S., Herman, R., Moore, G. E., & Silverman, S. 1962, ApJ, 135, 277
Bernath, P. F. 2017, JQSRT, 186, 3
Bielska, K., Cygan, A., Konefał, M., et al. 2021, OExpr, 29, 39449
Bielska, K., Kyuberis, A. A., Reed, Z. D., et al. 2022, PhRvL, 129, 043002
Bogey, M., Demuynck, C., Destombes, J. L., & Lapauw, J. M. 1986, JPhE, 19, 520
Bordet, B., Kassi, S., & Campargue, A. 2021, JQSRT, 260, 107453
Borkov, Y. G., Solodov, A. M., Solodov, A. A., et al. 2020, JQSRT, 253, 107064
Bowesman, C. A., Mizus, I. I., Zobov, N. F., et al. 2023, MNRAS, 519, 6333
Brown, L. R., & Toth, R. A. 1985, OSAJB, 2, 842
Campargue, A., Karlovets, E.-V., & Kassi, S. 2015, JQSRT, 154, 113
Chubb, K. L., Joseph, M., Franklin, J., et al. 2018, JQSRT, 204, 42
Chung, C.-Y., Ogilvie, J. F., & Lee, Y.-P. 2005, JPCA, 109, 7854
Cooper, D. L., & Kirby, K. P. 1987, JChPh, 87, 424
Coxon, J. A., & Hajigeorgiou, P. G. 2004, JChPh, 121, 2992
Coxon, J. A., & Hajigeorgiou, P. G. 2013, JQSRT, 116, 75
Császár, A. G., Czak, G., Furtenbacher, T., & Mátyus, E. 2007, Ann. Rep. Comp. Chem., 3, 155
Császár, A. G., & Furtenbacher, T. 2011, JMoSp, 266, 99
Császár, A. G., Furtenbacher, T., & Árendás, P. 2016, JPCA, 120, 8949
Cygan, A., Wcisło, P., Wójtewicz, S., et al. 2019, OExpr, 27, 21810
Cygan, A., Wójtewicz, S., Kowzan, G., et al. 2016, JChPh, 144, 214202
de Kok, R. J., Brogi, M., Snellen, I. A. G., et al. 2013, A&A, 554, A82
Devi, V. M., Benner, D. C., Smith, M. A. H., & Rinsland, C. P. 1998, JQSRT, 60, 815
Dixon, T. 1977, PhD thesis, University of Wisconsin
Duley, W. W., & Williams, D. A. 1992, MNRAS, 257, P13
Eng, R. S., Kildal, H., Mikkelsen, J. C., & Spears, D. L. 1974, ApPhL, 24, 231
Esteki, K., Predoi-Cross, A., Povey, C., et al. 2017, JQSRT, 203, 309
Evenson, K. 1995, Proc. of the 52nd Okazaki Conf.
Farrenq, R., Guelachvili, G., Sauval, A. J., Grevesse, N., & Farmer, C. B. 1991, JMoSp, 149, 375
Furtenbacher, T., Arendás, P., Mellau, G., & Császár, A. G. 2014, NatSR, 4, 4654
Furtenbacher, T., Coles, P. A., Tennyson, J., et al. 2020, JQSRT, 251, 107027
Furtenbacher, T., & Császár, A. G. 2012a, JQSRT, 113, 929
Furtenbacher, T., & Császár, A. G. 2012b, JMoSt, 1009, 123
Furtenbacher, T., Császár, A. G., & Tennyson, J. 2007, JMoSp, 245, 115
Furtenbacher, T., Szabó, I., Császár, A. G., et al. 2016, ApJS, 224, 44
Furtenbacher, T., Szidarovszky, T., Fábri, C., & Császár, A. G. 2013a, PCCP, 15, 10181
Furtenbacher, T., Szidarovszky, T., Mátyus, E., Fábri, C., & Császár, A. G. 2013b, JCTC, 9, 5471
Gamache, R. R., Vispoel, B., Rey, M., et al. 2022, Icar, 378, 114947
Gendriesch, R., Lewen, F., Klapper, G., et al. 2009, A&A, 497, 927
George, T., Saupe, S., Wappelhorst, M. H., & Urban, W. 1994, ApPhB, 59, 159
George, T., Wu, B., Dax, A., Schneider, M., & Urban, W. 1991, ApPhB, 53, 330
Gilbert, S. L., & Swann, W. C. 2002, Carbon Monoxide Absorption References for 1560 nm to 1630 nm Wavelength Calibration: SRM 2514 (12C16O) and SRM 2515 (13C16O), NIST Special Publication 260-146, National Institute of Standards and Technology, https://www.nist.gov/system/files/documents/srm/SP260-146.PDF
Goldberg, L., & Müller, E. A. 1953, ApJ, 118, 397
Goorvitch, D. 1994, ApJS, 95, 535
Gordon, I. E., Rothman, L. S., Hargreaves, R. J., et al. 2022, JQSRT, 277, 107949
Gordon, I. E., Rothman, L. S., Hill, C., et al. 2017, JQSRT, 203, 3
Gordy, W., & Cowan, M. 1957, BAPS, 2, 212
Gredel, R., Lepp, S., & Dalgarno, A. 1987, ApJL, 323, L137
Guelachvili, G. 1973, OptCo, 8, 171
Guelachvili, G. 1979, JMoSp, 75, 251
Guelachvili, G., de Villeneuve, D., Farrenq, R., Urban, W., & Verges, J. 1983, JMoSp, 98, 64
Hase, F., Wallace, L., McLeod, S. D., Harrison, J. J., & Bernath, P. F. 2010, JQSRT, 111, 521
Helminger, P., De Lucia, F. C., & Gordy, W. 1970, PhRvL, 25, 1397
Henningsen, J., Simonsen, H., Mgelberg, T., & Truds, E. 1999, JMoSp, 193, 354
Herzberg, G., & Rao, K. N. 2004, JChPh, 17, 1099
Hinz, A., Wells, J. S., & Maki, A. G. 1987, ZPhyD, 5, 351
Jones, G., & Gordy, W. 1964, PhRv, 135, 295
Jones, H. R. A., Pavlenko, Y., Viti, S., et al. 2005, MNRAS, 358, 105
Kildal, H., Eng, R. S., & Ross, A. H. M. 1974, JMoSp, 53, 479
Kowzan, G., Stec, K., Zaborowski, M., et al. 2017, JQSRT, 191, 46
Krasnopolsky, V. A. 2014, Icar, 228, 189
Krupenie, P. H. 1966, The Band Spectrum of Carbon Monoxide NBS NSRDS 5, National Bureau of Standards, doi:10.6028/NBS.NSRDS.5
Kurucz, R. L., Hubeny, I., Stone, J. M., MacGregor, K., & Werner, K. 2009, in AIP Conf. Proc. 1171, Recent Directions in Astrophysical Quantitative Spectroscopy and Radiation Hydrodynamics, ed. I. Hubeny (Melville, NY: AIP), 43
Li, G., Gordon, I. E., Rothman, L. S., et al. 2015, ApJS, 216, 15
Li, Y., Buenker, R., & Hirsch, G. 1998, AcTC, 100, 112
Lowry, E. F. 1924, JOSA, 8, 647
Mäder, H., Guarnieri, A., Doose, J., et al. 1996, JMoSp, 180, 183
Maki, A. G., Wells, J. S., & Jennings, D. A. 1990, JMoSp, 144, 224
Malathy Devi, V., Benner, D. C., Smith, M. A. H., Rinsland, C. P., & Mantz, A. W. 2002, JQSRT, 75, 455
Malathy Devi, V., Predoi-Cross, A., Chris Benner, D., et al. 2004, JMoSp, 228, 580
Mantz, A. W., & Maillard, J.-P. 1974, JMoSp, 53, 466
Mantz, A. W., Nichols, E. R., Alpert, B. D., & Rao, K. N. 1970, JMoSp, 35, 325
Markov, V. N., Golubiatnikov, G. Y., Savin, V. A., et al. 2002, JMoSp, 212, 1
Medvedev, E. S., & Ushakov, V. G. 2022, JQSRT, 288, 108255
Meshkov, V. V., Ermilov, A. Y., Stolyarov, A. V., et al. 2022, JQSRT, 280, 108090
Meshkov, V. V., Stolyarov, A. V., Ermilov, A. Y., et al. 2018, JQSRT, 217, 262
Mishra, A. P., Shetty, B. J., & Kshirsagar, R. J. 2005, JMoSp, 232, 296
Mondelain, D., Sala, T., Kassi, S., et al. 2015, JQSRT, 154, 35
Nakai, N., & Kuno, N. 1995, PASJ, 47, 761
National Academies of Sciences, Engineering and Medicine 2015, Frequency Allocations and Spectrum Protection for Scientific Uses (Washington, DC: National Academies Press)
Ngo, N. H., Landsheere, X., Pangui, E., et al. 2014, JQSRT, 149, 285

Nishiyama, A., Kowzan, G., Charczun, D., Trawiński, R. S., & Masłowski, P. 2020, ChJCP, 33, 23
Nolt, I. G., Radostitz, J. V., DiLonardo, G., et al. 1987, JMoSp, 125, 274
Ogilvie, J. F., Cheah, S.-L., Lee, Y.-P., & Sauer, S. P. A. 2002, Theor. Chem. Acc, 108, 85
Pastorek, A., Civiš, S., Clark, V. H. J., Yurchenko, S. N., & Ferus, M. 2021, JQSRT, 262, 107521
Picqué, N., & Guelachvili, G. 1997, JMoSp, 185, 244
Plyler, E. K., Blaine, L. R., & Connor, W. S. 1955, JOSA, 45, 102
Pollock, C. R., Petersen, F. R., Jennings, D. A., Wells, J. S., & Maki, A. G. 1983, JMoSp, 99, 357
Rank, D., Pierre, A., & Wiggins, T. 1965a, JMoSp, 18, 418
Rank, D. H., Eastman, D. P., Rao, B. S., & Wiggins, T. A. 1961, JOSA, 51, 929
Rank, D. H., Pierre, S., & Wiggins, A. G. 1965b, JMoSp, 18, 418
Roh, W. B., & Rao, K. N. 1974, JMoSp, 317
Rosenblum, B., Nethercot, A. H., & Townes, C. H. 1958, PhRv, 109, 400
Schneider, M., Evenson, K. M., Vanek, M. D., et al. 1989, JMoSp, 135, 197
Schneider, M., Wells, J. S., & Maki, A. G. 1990, JMoSp, 139, 432
Sokoloff, D. R., Sanchez, A., Osgood, R. M., & Javan, A. 1970, ApPhL, 17, 257
Swann, W. C., & Gilbert, S. L. 2002, OSAJB, 19, 2461
Tan, Y., Wang, J., Zhao, X.-Q., Liu, A.-W., & Hu, S.-M. 2017, JQSRT, 187, 274
Tashkun, S. A., Velichko, T. I., & Mikhailenko, S. N. 2010, JQSRT, 111, 1106
Tennyson, J., Bernath, P. F., Brown, L. R., et al. 2009, JQSRT, 110, 573
Tennyson, J., Bernath, P. F., Brown, L. R., et al. 2010, JQSRT, 111, 2160
Tennyson, J., Bernath, P. F., Brown, L. R., et al. 2013, JQSRT, 117, 29
Tennyson, J., Bernath, P. F., Brown, L. R., et al. 2014a, JQSRT, 142, 93
Tennyson, J., Bernath, P. F., Brown, L. R., et al. 2014b, Pure Appl. Chem., 86, 71
Tennyson, J., Furtenbacher, T., Yurchenko, S. N., & Császár, A. G. 2024, JQSRT, 316, 108902
Tóbiás, R., Furtenbacher, T., Császár, A. G., et al. 2018, JQSRT, 208, 152
Tóbiás, R., Furtenbacher, T., Tennyson, J., & Császár, A. G. 2019, PCCP, 21, 3473
Todd, T. R., Clayton, C. M., Telfair, W. B., McCubbin, T. K., & Pliva, J. 1976, JMoSp, 62, 201
Varberg, T. D., & Evenson, K. M. 1992, ApJ, 385, 763
Vázquez, G. J., Amero, J. M., Liebermann, H. P., & Lefebvre-Brion, H. 2009, JPCA, 113, 13395
Velichko, T. I., Mikhailenko, S. N., & Tashkun, S. A. 2012, JQSRT, 113, 1643
Velichko, T. I., Mikhailenko, S. N., & Tashkun, S. A. 2013, JQSRT, 116, 196
Wang, J., Hu, C.-L., Liu, A.-W., et al. 2021, JQSRT, 270, 107717
Wappelhorst, M. H., Saupe, S., Meyer, B., et al. 1997, JMoSp, 181, 357
Weinberg, J., Fishburne, E., & Rao, K. 1965, JMoSp, 18, 428
Wells, J. S., Hinz, A., & Maki, A. G. 1985, JMoSp, 114, 84
Wilson, R. W., Jefferts, K. B., & Penzias, A. A. 1970, ApJL, 161, L43
Winnewisser, G., Belov, S. P., Klaus, T., & Schieder, R. 1997, JMoSp, 184, 468
Winnewisser, M., Winnewisser, B. P., & Winnewisser, G. 1985, in Millimeter and Submillimeter Wave Spectroscopy in the Laboratory and in the Interstellar Medium, ed. G. H. F. Diercksen, W. F. Huebner, & P. W. Langhoff (Dordrecht: Springer), 375
Wójtewicz, S., Stec, K., Masłowski, P., et al. 2013, JQSRT, 130, 191
Yardley, J. T. 1970, JMoSp, 35, 314
Yoshida, T., & Sasada, H. 1992, JMoSp, 153, 208